Virology 452-453 (2014) 310–323

Contents lists available at ScienceDirect

Virology

journal homepage: www.elsevier.com/locate/yviro

Static and dynamic protein phosphorylation in the Vaccinia virion

J. Matson [a], W. Chou [b], T. Ngo [b], P.D. Gershon [b,*]

[a] University of North Carolina, Chapel Hill, NC, United States
[b] Department of Molecular Biology and Biochemistry, UC-Irvine, Irvine, CA 92697, United States

ARTICLE INFO

Article history:
Received 31 October 2013
Returned to author for revisions
2 December 2013
Accepted 17 January 2014
Available online 25 February 2014

Keywords:
Vaccinia
Virion
Phosphorylation
Phosphoprotein
Mass spectrometry
Kinase

ABSTRACT

To the best of our knowledge, two phosphorylation sites have been reported previously, among 11 known Vaccinia virus phosphoproteins. Here, via phosphopeptide mass spectrometry, up to 189 phosphorylation sites were identified among 48 proteins in preparations of purified Vaccinia mature virus (MV). 8.5% of phospho-residues were pTyr. Viral phosphoproteins were found in diverse functional classes, including structural proteins, membrane proteins and RNA polymerase subunits. Among the nine identified membrane phosphoproteins, the sites in just one, namely A14L, were deduced to be internal with respect to the accompanying membrane. Examination of sites in known substrates of the Vaccinia-encoded protein kinase VPK2, indicated VPK2 to be a proline-dependent kinase. The MV phosphoproteome was enriched in potential substrates of cellular kinases belonging to the CDK2/CDK3, CK2, and p38 groups. Quantitative mass spectrometry identified several sites that became phosphorylated during intravirion kinase activation *in vitro*, each showing one of two distinct pH-dependency profiles.

Introduction

More than 40 years has passed since the first demonstration of phosphoproteins in the Vaccinia virion (Rosemond and Moss, 1973; Sarov and Joklik, 1972), yet in the interim only a handful of Vaccinia phosphoproteins and even fewer phosphorylation sites therein have been reported. With so little known of phosphorylation targets in Vaccinia proteins, it seems necessary to briefly recap the entire 40 years: Accordingly, from the early finding that virion uncoating (using non-ionic detergent plus sulfhydryl reducing agent) in the presence of γ^{32}P-ATP led to the incorporation of ^{32}P into hot TCA precipitable material (Paoletti and Moss, 1972), initial studies focused largely on protein kinase activity present within the virion. This activity could phosphorylate endogenous proteins (within the virion core, mainly of low molecular weight) or exogenous substrates (histones, protamine), with specificity for Ser and Thr residues (Paoletti and Moss, 1972). Protein kinase activity could be solubilized from whole virions (Kleiman and Moss, 1973) or virion cores and, with purification, core-derived kinase was increasingly dependent upon the virion membrane fraction (Kleiman and Moss, 1973) or acceptor proteins therefrom (Kleiman and Moss, 1975b). Kinase activity was associated with a polypeptide of 62 kDa molecular weight (Kleiman and Moss, 1975b) with an alkaline pH optimum (Kleiman and Moss, 1975a; Paoletti and Moss, 1972), and was activated by protamine (Kleiman and Moss, 1975a). Substrates were phosphorylated at (mainly) serine and threonine residues (Kleiman and Moss, 1975a).

Subsequently, Vaccinia gene B1R was shown to encode a 34.2 kDa essential protein with homology to the catalytic domains of numerous protein kinases (Howard and Smith, 1989; Lin et al., 1992; Rempel and Traktman, 1992; Traktman et al., 1989). Bacterially-expressed GST-B1R could phosphorylate exogenous substrates including casein and histones H1, H2B and H3, recombinant 6His-B1R at Ser/Thr residues (Mercer and Traktman, 2005) and it's own GST moiety at Thr residues (Banham and Smith, 1992; Lin et al., 1992; Rempel and Traktman, 1992). B1R kinase (also referred to as vaccinia protein kinase 1, or VPK1) was shown to be associated with the virus particle—mainly the core (Banham and Smith, 1992; Lin et al., 1992). In core extracts, however, the chromatographic separation of bulk casein kinase activity from endogenous B1R protein indicated the presence of additional kinases in the particle (Lin et al., 1992). The major portion of core kinase activity was subsequently attributed to a second essential S/T protein kinase ("VPK2") encoded by Vaccinia late gene F10L (Lin and Broyles, 1994). This 50-kDa polypeptide could phosphorylate α-casein primarily at Ser residues as well as a casein kinase I-specific peptide substrate, myelin basic protein, and itself through autophosphorylation (Mercer and Traktman, 2005). VPK2 also binds phosphoinositides (Punjabi and Traktman, 2005). VPK2 expression and autophosphorylation occur late during infection (Punjabi and Traktman, 2005), and VPK2 is tightly associated with membranes (Punjabi and Traktman, 2005). While VPK1 is structurally related to a group of cellular kinases (the "VRKs" (Nezu et al., 1997)), the only known phylogenetic relatives of VPK2 are homologs from other poxviruses (Punjabi and Traktman, 2005).

* Corresponding author. Tel.: +1 949 824 9606.
E-mail address: pgershon@uci.edu (P.D. Gershon).

0042-6822/$ - see front matter © 2014 Elsevier Inc. All rights reserved.
http://dx.doi.org/10.1016/j.virol.2014.01.012

Roles of VPK1 and VPK2 are likely complex: Both kinases are essential for Vaccinia viability (Jacob et al., 2011; Lin and Broyles, 1994; Rempel and Traktman, 1992). VPK1 is expressed early during infection (Rempel and Traktman, 1992) and can later be found in viral factories (Banham and Smith, 1992) and within the virion. Temperature-sensitive (ts) mutants in VPK1 arrest at or prior to the DNA replication stage of infection under non-permissive conditions (Rempel and Traktman, 1992; Traktman et al., 1989), and VPK1 may have an additional role in Vaccinia intermediate transcription by relieving the cellular inhibition of intermediate gene promoters (Ibrahim et al., 2013). ts Mutants in VPK2, on the other hand, are blocked in virion morphogenesis at an early stage of virion assembly (Wang and Shuman, 1995), and VPK2's catalytic activity is required to overcome this block (Szajner et al., 2004). VPK2 contributes to a complex of seven proteins required for the earliest stages of virion morphogenesis (namely the association of membranes and viroplasm) (Szajner et al., 2004).

In addition to the roles of VPK1 and 2 defined via genetic approaches (above), biochemical experiments have indicated that protein phosphorylation events in the virion core, at the very outset of infection, activate early gene transcription within the infecting virus particle. Specifically, while the activation of purified cores *in vitro* is associated with a ~2 min lag in the start of early gene transcription, this lag is abolished by the pre-incubation of cores with ATP. Moreover, protein phosphorylation progresses linearly during this ~2 min window without a lag (Moussatche and Keller, 1991). At least 12 distinct virion proteins were shown to become phosphorylated during this time window according to SDS-PAGE autoradiograms (Moussatche and Keller, 1991), with the majority of ^{32}P label incorporated into low molecular weight proteins. By pre-incubation at pH 7.0 instead of pH 8.5 and in the presence of limiting ATP, the lag was restored and two proteins (70, 80 kDa) specifically failed to became phosphorylated (Moussatche and Keller, 1991).

In addition to the two identified protein kinases (above), Vaccinia encodes (Guan et al., 1991) and encapsidates (Liu et al., 1995) a dual specificity protein phosphatase ("VH1", the prototypic member of the dual-specificity phosphatase class). Upon repression of VH1 expression, virions are produced normally during infection but with greatly reduced infectivity due to their inability to transcribe early genes (Liu et al., 1995). A 1.32 Å crystal structure shows VH1 to be a homodimer (Koksal et al., 2009).

Which Vaccinia proteins are known to be phosphorylated? Table 1 lists the eleven Vaccinia proteins (and two residues) shown to be phosphorylated prior to the current study, and Table S1 summarizes in detail prior studies of Vaccinia protein phosphorylation, along with associated description (Supplementary introduction). With regard to host (cellular) protein substrates: Proteins S2 and Sa of the 40S ribosomal subunit have been identified as VPK1 substrates (Banham et al., 1993). In addition, a story is emerging in which kinases/phosphatase carried by the particle may have roles in influencing cellular signaling, specifically innate defenses early during infection (Supplementary introduction).

Here, we have characterized the phosphoproteome of the Vaccinia virus particle identifying, conservatively, 189 sites of phosphorylation among 48 proteins. We have also characterized VPK2's consensus binding site, along with candidate cellular kinases contributing to the virion phosphoproteome. Further, we have examined dynamic changes in phosphorylation upon activation of the virus particle *in vitro* and the pH-dependency thereof. Our data address and extend a number of the above-described prior observations of Vaccinia protein phosphorylation.

Results

MV proteome: A meta-analysis

Three MS studies of the Vaccinia virion proteome have been published (Chung et al., 2006; Resch et al., 2007; Yoder et al., 2006). As a baseline for investigation of the virion phosphoproteome (below), we assayed the proteome of our own preparation of mature virus (MV) of Vaccinia strain WR. Table S2 shows a comparison of the four resulting virion proteome studies (three of strain WR, one Copenhagen strain) and Fig. 1 shows a meta-analysis of Table S2. Of the 217 unique protein accessions comprising the current UniProt reference proteome for Vaccinia strain WR, 53 were unanimously identified as MV-associated in all four studies, 112 were unanimously not found to be virion-associated in any of the four MS studies. The latter group of proteins includes G5R, a FEN1-like nuclease (Senkevich et al., 2009), which was found to be virion-associated by immunoblotting (da Fonseca et al., 2004), a technique that is arguably more sensitive than MS. 20 additional Vaccinia proteins were found by just one of the four groups of investigators, and 32 further Vaccinia proteins by two or three groups. The above numbers attest to a core proteome whose abundance is above the minimum threshold for detection by all groups combined with, perhaps, differential sensitivity/analysis depth thresholds among groups for low abundance virion proteins, and/or an overlapping fields of contaminants between virus preparations.

MV phosphoproteome: Approach and thresholding

We next investigated protein phosphorylation in the Vaccinia virion. Fig. 2 summarizes the strategies implemented. Overall, a "bottom-up" approach was taken, in which purified Vaccinia MV was disaggregated prior to tryptic digestion and enrichment for phosphopeptides. Peptides and phosphorylation sites were then identified via nanoLC-MS/MS. In some experiments, prior to disaggregation and digestion, aliquots of purified MV were "activated" by

Table 1
Eleven vaccinia proteins shown to be phosphorylated prior to the current MS-based study.

Protein	Packaged?	Residue(s) phosphorylated in infected cells
F17R	Y	pSer
A17L	Y	pSer, pThr and pTyr; Y203
A14L	Y	Ser residues; S85
F10 (VPK2)	Y	Thr residues
A30L	Y	Ser residues
G7L	Y	Ser residues
H5R	Y	Thr residues. Recombinant H5R is phosphorylated by recombinant VPK1 *in vitro* at Thr84 and Thr85
A13	Y	Ser residues, (Ser 40?)
I3	Y	Ser residues
A11R	Probably	
E8R	Y	

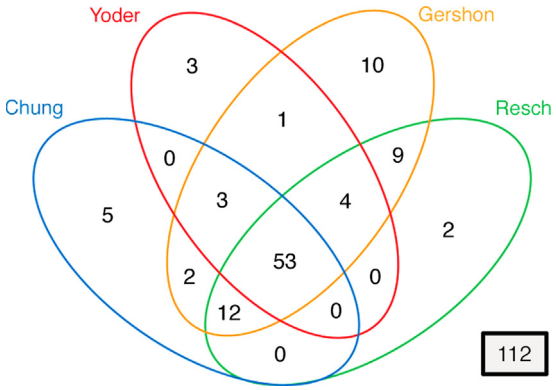

Fig. 1. Venn diagram showing overlaps between Vaccinia MV proteomes discovered in four separate MS studies, in terms of numbers of Vaccinia proteins commonly identified. One hundred twelve (black box) indicates the number of proteins from the current Vaccinia reference proteome not found to be virion-associated in any of the four studies.

incubation under conditions intended to either uncoat or simultaneously uncoat/activate intravirion kinases. In such cases, the tryptic digestion products of activated virions and associated controls were differentially labeled with stable isotopes prior to pooling, phosphopeptide enrichment and nanoLC-MS/MS with quantitative analysis of isotopically offset mass clusters in mass spectra at the precursor-peptide level (Chou et al., 2012). In order to maximize the diversity of phosphopeptides identified, as well as confidence in the localization of phosphate groups within phosphopeptides, replicate experiments were accompanied by a "strategy of variation" employing variously sized aliquots of MV, a variety of phosphopeptide enrichment techniques (phases, supports, strategies) and elution solvents (Fig. 2), two distinct mass spectrometers, various data-dependent spectral acquisition strategies and peptide dissociation methods inside the mass spectrometer, and various database search parameters (tryptic or semi-tryptic cleavage specificity, ±deamidation, ±isotope error mode (0-^{13}C or 1-^{13}C): All Mascot search, report and export parameters are given in Supplementary methods, Table S6). We chose the most conservative scoring thresholds (Table S6) for our final dataset in order to minimize "noise" that may arise from ambiguous phosphosite localization within peptides whose identification as phosphopeptides might nonetheless be considered confident (see Table S6 legend). Our chosen threshold criterion was 1% homology FDR (false-discovery rate in target-decoy searches, see "Materials and methods" section and legend to Table S6). A 1% threshold can be regarded as an indication of 99% statistical confidence that peptides were correctly identified. Via use of a stringent threshold, a number of high-confidence phosphopeptides may have been excluded from the final dataset whose site localization within the peptide was less confident.

Overall interpretation of virion phosphopeptide data

Table S3 shows the complete dataset of virion-derived phosphopeptides exceeding the conservative 1% homology FDR threshold, from 12 analyses of seven phosphopeptide samples. In Table S4, the dataset of Table S3 has been condensed to show just one row per identified phosphopeptide positional isomer. Filtering criteria used in the condensation of Tables S3 and S4 are given in "Supplementary methods". Fig. S1 shows the phosphopeptides of Table S4 aligned against complete protein sequences of the Vaccinia proteome. The conservative MV phosphoproteome (Table S4, Fig. S1) covered 189 sites of phosphorylation among 48 Vaccinia virus accessions. Since the seven phosphopeptide samples included two from experiments designed to activate the virion-packaged kinases (see below), then the listings in Tables S3 and S4 may include a few sites detected only as a result of their having become phosphorylated during *in vitro* activation.

Among the 48 Vaccinia accessions, 27 were shared with the 53-member consensus virion proteome (above), and 10 were from the 112-member group of proteins not previously detected in the MV proteome by any of the four sets of investigators (above). These 10 included: Uncharacterized protein 18 (from the left end of the genome); N2L/BCL2-like; A1L/VLTF2; A23R/VITF3; A44L (3 beta-hydroxysteroid dehydrogenase/Delta 5→4-isomerase); A47L (inferred); B8R (soluble interferon gamma receptor); B13R/SPI2; B18R (ANK repeat protein) and small open reading frame (ORF) YVDA (Table S2). From the perspective of Vaccinia lifecycle, none of these 10 has an obvious role within the infectious mature virion.

Alternative sites of phosphorylation vs. localization ambiguities

The experiments of this study were tasked with not only the confident identification of phosphopeptides, but also the confident localization of phosphorylated residue(s) therein. For phosphopeptides containing multiple potential acceptor sites, scoring methods for the accuracy of phosphate localization remain a subject of debate in the field (Chalkley and Clauser, 2012; Fermin et al., 2013). Here, phospho-residue assignments were scored according to Mascot's implementation of reference (Savitski et al., 2011) based on numbers of distinguishing fragmentation ions between possible phospho-positional isomers ("Materials and methods"). Resulting scores, referred to here as "site_analysis confidence" (SAC), represent confidence (%) that a given site is the correct one. In our conservatively-thresholded phosphopeptide dataset, we adopted a liberal interpretation, namely that the listed positional isomers were, except when arising from the same Mascot query of the same precursor ion in the same mass spectrum, genuinely alternative phosphate positions. Reasons for this interpretation are expounded in Supplementary materials.

Proportion of pSer, pThr and pTyr sites in the MV phosphoproteome

Of the 189 phosphorylation sites in the conservatively-thresholded MV phosphoproteome, 121, 151 and 16 sites (64.4%, 27.1% and 8.5%) represented pSer, pThr and pTyr residues, respectively. The content of pTyr was markedly higher than the 0.05% estimate for tyrosine phosphorylation in cellular organisms (Hunter, 1998; Hunter and Sefton, 1980; Mann et al., 2002). Those estimates, however, pre-date recent advances in phosphopeptide enrichment and MS. Moreover, the Vaccinia kinase VPK2 shows specificity for pTyr (Betakova et al., 1999; Derrien et al., 1999; Szajner et al., 2004), and Vaccinia proteins may be predisposed to intersect with cellular signal transduction and regulation pathways.

Some phosphorylation sites, at least, are only partially occupied in the virion

To assay for partial occupancy of phosphorylation sites in the virion, peptides in the TiO_2 flowthrough fraction from experiment "Kinase2" were subjected to SCX (strong cation exchange) fractionation (Fig. 2). In the resulting fractions, non-phosphorylated counterparts were found for 86 of the 233 phosphopeptide species in the conservatively-thresholded MV phosphoproteome (Table S4). These represented 77 of the 189 distinct phosphorylation sites therein (including sites for which a non-phospho counterpart was found to one but not all nested or overlapping phosphopeptides). The presence of non-phosphorylated counterparts to multiply-phosphorylated phosphopeptides indicated that, in some protein molecules, multiple sites were simultaneously empty. Reasons for not finding greater numbers of non-phosphorylated counterparts might include 100% site occupancy at other sites, the absence of

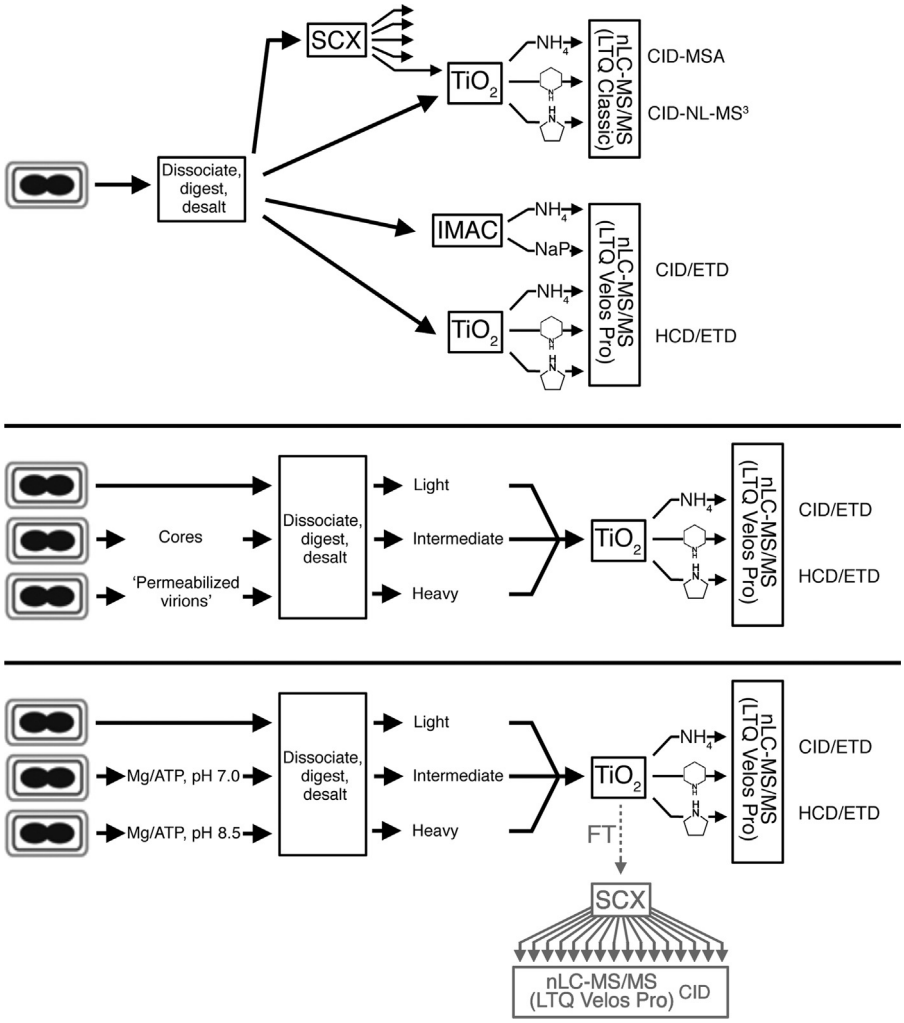

Fig. 2. Diversity of experimental workflows. "Dissociate, digest, desalt" represents the urea-based dissolution of virions and tryptic digestion of virion proteins to peptides. *Upper panel*: MV phosphoproteome experiments without quantitation. Virion phosphopeptides were isolated via either TiO_2-based enrichment directly, immobilized metal affinity chromatography (IMAC), or strong cation exchange (SCX) prior to TiO_2-based enrichment. "NaP"=sodium phosphate buffer. Phosphopeptides were analyzed using either an LTQ Classic or an LTQ Velos Pro mass spectrometer. Instrument methods for the LTQ Classic were based on a combination of collision-induced dissociation (CID) with either multistage activation (MSA) or neutral loss MS^3 ($NL\text{-}MS^3$). Instrument methods for the LTQ Velos Pro were based on either alternating CID and electron transfer dissociation (ETD) scans, or alternating higher-energy collisional dissociation (HCD) and ETD scans. *Center panel*: Virions were treated under two alternative sets of conditions designed to activate them to an early transcription-ready state. Peptides generated from the activated (and a third, unactivated) aliquots of virus were subjected to differential stable isotope-labeling ("light", "intermediate", "heavy") prior to mixing of the labeled samples, phosphopeptide enrichment and nanoLC-MS/MS. *Lower panel*: Virions were treated, at two distinct pHs, under conditions expected to activate the intra-virion kinase(s) prior to stable isotope labeling, phosphopeptide enrichment and quantitative nanoLC-MS/MS. *Gray*: Non-phosphopeptide fractionation: The TiO_2 flow-through fraction from a kinase activation experiment was bound to SCX and 16 salt fractions were each subjected to nanoLC-MS/MS. Peptides identified via the 16 resulting database searches were combined into a single "virion non-phosphopeptide" dataset.

an exhaustive search, and/or technical factors such as sensitivity of the analysis and peptide ionizability.

MV phosphoproteome, protein-by-protein

Within the 48-protein conservatively-thresholded MV phosphoproteome, phosphorylation was most apparent among membrane proteins (9 proteins), structural/virosomal proteins (11 proteins including F17R) and proteins involved in early transcription (8 proteins, mainly RNA polymerase subunits). These and other protein groups in the MV phosphoproteome are discussed below with reference to Table S4 and Fig. S1, and their consistency with prior studies is considered in "Discussion" section.

Membrane proteins

The phosphorylation of nine membrane proteins was detected in the conservative dataset. Seven of the nine were found in the MV proteome (unanimously, Table S2), the two exceptions being proteins A9L and A28L, which were not detected in the Copenhagen strain analysis (Yoder et al., 2006). The nine membrane proteins included: *A14L*: The phosphorylation of three Ser residues was detected, in a cluster at the C-terminus. This region of A14L is considered to be *internal* with respect to the accompanying membrane (Condit et al., 2006). *A17L*: Four phosphorylation sites (pSer:3; pTyr:1) were detected, towards the N- and C-termini of the protein. Both ends appear to be *external* with respect to the accompanying membrane (Condit et al., 2006). *A13L*: The phosphorylation of six sites was detected within this 70 aa membrane protein (pSer:5; pThr:1), spanning the region from aa40 to aa69. This region is likely be *external* with respect to the accompanying membrane (Condit et al., 2006). *A26L*: The phosphorylation of nine residues was detected in phosphopeptides from protein A26L (pSer:4; pThr:3; pTyr:2). The membrane topology of A26L is unclear (Condit et al., 2006). *A9L*: The phosphorylation of 6 Ser residues was detected in A9L, all of which cluster towards the C-terminus. Scoring of replicates of each positional isomer suggests,

with high probability, that at least some of the 6 Ser residues are bona fide alternative sites, albeit no confirmatory multiply-phosphorylated peptides were found. The C-terminal end of A9 would be *external* with respect to the accompanying membrane (Condit et al., 2006). *L1R*: A single pThr was detected in protein L1R, located close to the protein N-terminus. This region would be *external* with respect to the accompanying membrane (Condit et al., 2006) and presumably in the vicinity of a known myristoyl group. *A28L*: One phosphorylation was detected in protein A28L (pSer at aa48). This residue would be either within the membrane-spanning region, or just to the *external* side of it (Condit et al., 2006). *H3L*: Five phosphorylation sites were detected within protein H3L (pSer:1, pThr:3; pTyr:1). Two pairs of sites (one located around aa20 and the other around aa193 of this 324 aa protein), are each likely to be alternate positions of a single phosphate since each pair represents alternative interpretations of a single Mascot query with equivalent SAC values. Nonetheless, the possibility that they could be co-chromatographing positional isomers cannot be discounted. The N-terminal 2/3 of H3L protein is likely *external* with respect to the accompanying membrane (Condit et al., 2006). *D8/CAHH*: This protein has up to six sites of phosphorylation (pSer:4; pThr:2) within the C-terminal 53% of the protein. This region would likely be *external* with respect to the accompanying membrane (Condit et al., 2006). Two of the three adjacent pSer in the region aa204–206 represent alternative interpretations of a single Mascot query with equivalent SAC values, in which pSer 205 could be an ambiguous call with pSer 204 and pSer 206 being real.

Irrespective of membrane protein topology (type I, type II and double membrane-spanning proteins were represented within the above group of 9 proteins), phosphorylation sites in just one protein (A14L) were internal with respect to the accompanying membrane. This indicated that the responsible kinase(s) may be compartmentalized in the immature or maturing virion, located to one side only of a morphological stage such as the crescent, or perhaps at the interface of IV with its external scaffold. In this regard, immunoEM of IV shows VPK2 localizing to the interior of the IV membrane (Szajner et al., 2004). Moreover, in infected cells, immunofluorescence microscopy shows VPK2 localizing to the perinuclear region, co-localizing with ER- and ERGIC-specific markers (Punjabi and Traktman, 2005). Notably, both A14L and A17L have been indicated to insert co-translationally into the ER (Rodriguez et al., 1997; Salmons et al., 1997).

Virosomal proteins

All members of the 7-member virosomal "assembly" complex involved in early virion morphogenesis (comprising proteins A30L, G7L, VPK2, A15L, D2L, D3R, J1R, (Szajner et al., 2004)) have been detected in MV (unanimously, Table S2). The MV phosphoproteome included three proteins from this complex, namely A30L, G7L and VPK2. *A30L*: Two phosphorylation sites were identified in protein A30L. They were positional isomers of a single phosphopeptide, and mapped towards the protein C-terminus. No multiply-phosphorylated peptides were available to confirm the presence of both sites, and while the two sites were not alternative interpretations of a single Mascot query, nonetheless, the site at Ser 69 appeared to score more confidently than the site at Ser 57 (Table S3, Mascot expectation score). *G7L*: Of the eight possible sites detected in G7L (pSer:2; pThr:6), all lay C-terminal to the two internal proteolytic processing sites (Condit et al., 2006), *i.e.* within the C-terminal 15 kDa segment known to remain associated with the virion core after processing (Condit et al., 2006). Within this segment, the 299–315 region of G7L protein contained a cluster of seven apparent phosphorylation sites (*T*DGAV*T*SPL*T*GNN*T*I*T*T). The presence of a diphosphopeptide and a triphosphopeptide in addition to monophosphopeptides (Tables S3 and S4) supported the existence of multiple phosphorylations in this cluster (Table S3). Nonetheless, it is considered possible that T314/T315 represent the ambiguous localization of a single site. *VPK2*: VPK2 phosphorylation was detected at three sites (two adjacent Ser, and one Tyr). The two pSer were each detected in six analyses, with similar frequency (Table S4), and each showed high confidence (Mascot expectation) scores and similar/high localization confidence ("Best SAC" values, Table S4). They are therefore regarded as alternative phosphorylation sites as opposed to localization ambiguity, though the latter cannot be discounted. The Tyr phosphorylation scored with lower confidence than did either pSer.

Phosphorylation was detected in a fourth protein *A11R*, generally considered to be virosomal with an early morphogenic role in viral crescent formation (though apparently not part of the 7-member complex). This protein, which was reported to not be encapsidated (Resch et al., 2005), was found in virion preparations by two groups (Table S2). In the current study, A11R phosphorylation was detected at two adjacent pSer (S55/S56) and one pThr (T92). S55/S56 are likely alternate candidate positions for a single site since they arose from the same Mascot query with the same expectation score and SAC (Table S3), and no confirmatory multi-phosphopeptides were detected.

Structural/processed proteins

In addition to the virosomal proteins above, some or all of which could have a structural role in Vaccinia MV, the phosphorylation of six major structural/processed proteins was detected in the MV phosphoproteome plus a protein (F17R) that has variously been described as structural. Within this group of seven proteins, A3L/p4b, A4L/p39 and A10L/p4a contained the greatest numbers of identified phosphorylation sites of any protein in the conservative dataset, namely 24, 15 and 11 apparent sites, respectively. Protein L4R/VP8 was not far behind with 8 sites. The relatively high count of phosphorylation sites identified in this group could have been technical in nature, attributable to the elevated abundance of these proteins in the virion (as indicated by phosphopeptide "frequency counting", Supplementary methods). Several Vaccinia structural proteins undergo proteolytic processing during virion maturation. These include, in addition to membrane and virosomal proteins A17L and G7L respectively (above), the major structural proteins A10L/p4a, A3L/p4b and L4R/VP8, and the processed protein A12L (Condit et al. (2006) and references therein). Phosphorylation sites were detected in each of these four proteins (Table S4).

Individually: *A10L/p4a* is proteolytically processed at two positions excising a central portion of the protein likely comprising aa616–697 (Condit et al., 2006; VanSlyke et al., 1991; VanSlyke et al., 1991). Four phosphorylation sites were detected within the packaged N-terminal 62 kDa region, along with two apparent clusters within the packaged C-terminal 23 kDa region (Fig. S1). The first of the latter two clusters comprised four apparent phosphorylation sites located between residues 732 and 748. Some of these could be ambiguous site localizations (from the presence of query groupings, Table S3), albeit the detection of diphosphopeptides (and triphosphopeptides in the 5% thresholded dataset, not shown) indicated that two or three, at least, of the four sites are real. No phosphorylation sites were detected within the excised (unpackaged) region of p4a. *A3L/p4b*: Up to 24 sites were detected in A3L/p4b (pSer:14; pThr:8; pTyr:2). This was the greatest number of phosphorylation sites detected within a single protein in the conservative dataset. Nonetheless, a couple of pairs of sites may be considered to be ambiguous localizations of a single site, namely, S19/20 and T537/Y544. Proteolytic processing

upon virus maturation removes a 6 kDa peptide from the N-terminus of A3L/p4b (Condit et al., 2006). The finding of a cluster of three pSer towards the N-terminus therefore indicated the presence of traces of IV in the MV preparation. *L4R/VP8*: Of the eight phosphorylation sites identified in L4R/VP8 (pSer:7; pTyr:1), some could be considered ambiguous such as S136/S137 (whose most likely assignment may be S136). Within the SYSSS cluster at position 216, the strongest SAC values were recorded at S216 and S220 (though phosphorylation at each of the Ser residues in this region cannot be discounted). A 4 kDa peptide is removed from the N-terminus of L4R/VP8 during proteolytic processing. However, all phosphorylation sites were found within the C-terminal (packaged) half of the protein. *A12L*: This processed protein (which is likely not a core structural protein) contains four apparent phosphorylation sites (S79 and T102/T103/S104). Within the latter cluster, the two most likely locations are T103 and S104 (since the two assignments to T102 are both split with the more confident and abundantly identified T103, as "query groups", Table S3). After removal of 6 kDa from the N-terminus of protein A12L by proteolytic processing (Condit et al., 2006), all identified phosphorylation sites would lie within the packaged C-terminal region.

In addition to the four proteins described above, three additional proteins were assigned to the "structural/processed proteins" group, namely, *A4L/p39*: Up to 15 phoshosites were identified in this major structural protein, (pSer:8; pThr:5; pTyr:2), located in an intensive patch towards the N-terminus, and also spread through the remainder of the protein. Within the cluster S14/S15/T16, S14/S15 represents localization ambiguity in which the phosphate is assignable to either residue. Within the cluster SSIYY starting at residue S19, S20 appears to be the most probable position with S19, Y22, Y23 being ambiguous localizations (Table S3). *E11L*: A single phosphosite was found in this MV core protein, namely a pSer adjacent to the C-terminal residue. *F17R*: Six phosphosites were detected in protein F17R (pSer:5; pThr;1). The five pSer clustered around closely-spaced PSSP and PSSPS motifs in the region spanning residues 52 to 65. By "frequency-counting" (Supplementary methods), F17R phosphopeptide VDKPSpSPACER was found to dominate the MV phosphoproteome overall, in absolute abundance (Tables S3 and S4). S52/53 and S61/62 could each be considered a pair of ambiguous sites since, for each isomer, some Mascot queries bifurcated to give alternative interpretations of identical queries and there were no high-scoring confirmatory multiply-phosphorylated peptides. Nonetheless, high-scoring queries also existed unequivocally selecting each one of these four phospho positions with high SAC values (apparently, distinguishing fragment ions were available in spectra in which the precursor ion was sufficiently abundant). It is therefore concluded that all four Ser residues are alternative sites of biological phosphate attachment via the liberal interpretation metric (above).

RNA polymerase and early transcription

Phosphorylation was detected in five subunits of the 8-Subunit Vaccinia RNA polymerase, including the two largest subunits (*J6R/RP147* and *A24R/RP132*—one site apiece, at Ser residues) as well as three smaller subunits (D7R/RP18, A5R/RP19 and E4L/RP30). One pSer was detected in *D7R/RP18*, while phosphorylation of *A5R/RP19* included a cluster of six (pSer:5; pThr:1) high scoring, apparently alternatively and multiply-phosphorylated sites between residues 40 and 60 of this 164 amino acid protein, in which S40 and S41 were likely ambiguous positions for a single phosphate. *E4L/RP30*, similarly, contained a cluster of sites (pSer:3; pThr:1) located towards the C-terminus of the protein. *H4L/RAP94*: This protein showed two pairs of adjacent sites (SS and ST) located around the center of the protein's linear sequence. While the former two may represent localization ambiguity (Table S3), the latter two were found within a diphosphopeptide and therefore appear to be simultaneously occupied. Of the two subunits of the Vaccinia early transcription factor (VETF) heterodimer: *D6R/ETF1* (VETF small subunit) showed a single site (pSer), close to the protein's C-terminus. The transcriptional ATPase *D11L/NTP1* also showed a single pSer.

A18R/H5R/G2R group

This complex serves in the regulation of late gene transcription (Black et al., 1998), and H5R has apparently unrelated roles in DNA replication and virion assembly. A18R and H5R are clearly virion-associated (Table S2), and *G2R* was detected in virion preparations by the Gershon group only. A single phosphorylation site was found in G2R within our MV preparation, namely a pThr at the penultimate residue of the protein. *H5R*: A total of nine sites (pSer:8; pThr:1) were detected scattered through the H5R protein. Of these, phosphorylation at S46/T47 could represent a localization ambiguity in which the favored alternative would be S46 (Table S3). We did not detect the phosphorylation of virion-associated H5R at the sites (Thr84/Thr85) found to be occupied after incubating recombinant H5R with recombinant VPK1 under *in vitro* kinase conditions (Brown et al., 2000). Phosphorylation was not detected in protein A18R.

REDOX pathway

Within the REDOX/sulfhydryl bond/thiol transfer-related proteome (comprising proteins O2L/GLRX1, G4L/GLRX2, E10R, A2.5L, F9L), phosphorylation was detected in just one protein, namely *A2.5L*. Three potential phosphosites were detected (pSer:1; pThr:2) located in a cluster towards N-terminus of this 76 residue protein, interleaving with the protein's two cysteines. All combinations of monophospho and diphosphopeptide were detected, in five distinct peptide backgrounds, providing clear evidence of multiple and alternative occupancies (with ambiguity in just one experiment, Table S4).

DNA metabolism

We detected the intravirion phosphorylation of just one protein with function in the DNA metabolism category, namely *K4L* (nicking enzyme). K4L contained an apparent cluster of up to six phosphosites (pSer:2; pThr:2; pTyr:2) in the Y381–T391 region (close to the protein C-terminus, Fig. S1). Three sites within the cluster 381-YSY represent, apparently, the ambiguous localization of a single phosphate. The cluster T388/S389/T391 also represents, most likely, the ambiguous location of a single phosphate whose most probable location is S389 (Table S3).

Proteinases

Vaccinia encodes contains two known proteinases, both shown to be virion-associated (Table S2). Phosphorylation was found, here, in both proteins. Within *G1L* (metalloproteinase), two sites were detected (both pSer), one towards the center of the protein and the other towards the C-terminus. Within *I7L* (core cysteine proteinase), A single site (pSer) was detected, located towards the center of the protein.

Defense

Phosphorylation was found within three proteins related to the combating of host defenses, namely: *C3L/VCP* (complement pathway inhibitor/complement control protein): Ours is the only group to have detected this protein in MV preparations (Table S2), and it contained a single phosphorylation (at pSer) being detected in the

protein. The remaining two defense proteins have not been detected in MV previously, by any group. These are: *B8R* (soluble gamma IFN receptor, one pSer); and *B13R/SPI2* (inhibits IL1beta-converting enzyme, one pThr).

Role in IV→MV transition, protein detected in MV

A single phosphopeptide was detected from protein *A6L* (a virion core protein with an essential role in virus maturation (Meng et al., 2007), which was detected in MV by some groups but not others, Table S2). This phosphopeptide contained two phosphosites, at residues Thr112 and Ser118.

Proteins of unknown function, previously detected in MV preparations

A single pThr was detected in protein *F8L*, which has been detected in MV preparations by all groups (Table S2). Four phosphosites were detected in protein *A19L*, which has been detected in MV preparations by some groups not others, Table S2 (pSer:3; pThr:1).

Other proteins of known function, not previously detected in MV preparations

Phosphorylation was found in three proteins that have not previously been detected in MV preparations by any group (Table S2). Two of them, with roles as transcription factors in the infected cell, are: *A23R/VITF3* (a single triphosphopeptide spanning S117/S118/Y122) and *A1L/VLTF2* (a single pSer). The third was *A44L/3BHS* (3 beta-hydroxysteroid dehydrogenase/Delta 5→4-isomerase), in which a single pSer was detected.

Proteins of unknown function, not previously detected in MV preparations

Phosphorylation was found in five proteins of unknown function that have not previously been detected in MV preparations by any group (Table S2). These were: *B18R* (ankyrin repeat-containing protein)—a single pTyr; *protein N2L* (bcl2-like)—a single pTyr; *A47L*—a single pSer; *V018* (predicted protein): a single triphosphopeptide (pSer:2; pTyr:1); and finally a small orf, namely *D orf A*, containing a single pSer.

Phosphorylation site analysis

Amino acid composition within phosphorylated regions

The phosphopeptides listed in Table S4 did not, by any means, fully cover each protein in which they were found. Possible technical reasons for this are typical of any MS experiment, and might be exacerbated by the range of protein and phosphopeptide abundances encountered in the virion (above). Partial coverage may also have been dictated by "hotspots" of biological phosphorylation. In a preliminary test for the latter, amino acid composition was calculated for the phosphopeptide contigs (Table S4) and their encompassing whole proteins and, for each of the 20 common amino acids, converted to a ratio of composition(contigs)/composition(whole proteins) (Fig. 3). The contigs were noticeably enriched for Ser and Pro residues with respect to their parental proteins, suggesting the occurrence of substantial Pro-dependent Ser phosphorylation among packaged phosphoproteins. Pro-bias may have resulted from these sites being resident within protein loops, which may be intrinsically Pro-rich, and/or substrate recognition by Pro-dependent kinases. Contigs were also enriched (to a lesser extent) for T, D, N and Q.

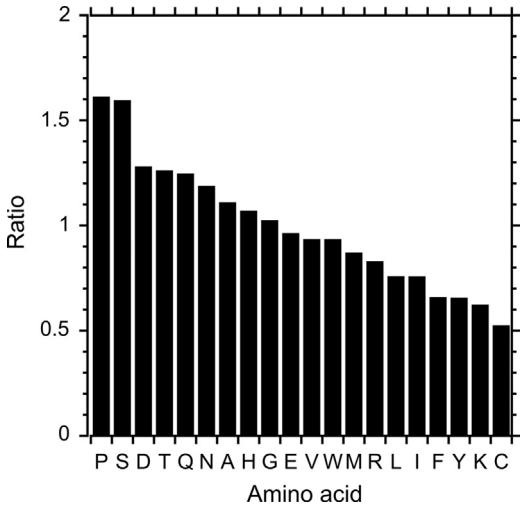

Fig. 3. Amino acid composition of phosphopeptide-containing contigs divided by that of their encompassing whole proteins, expressed as a ratio for each of the 20 common amino acids. A higher ratio for a given residue type indicates its enrichment in phosphopeptide-containing contigs. Despite the contigs not perfectly bracketing phosphorylated regions (contig ends being defined by trypsin cleavage sites), they were clearly enriched for Ser and Pro with respect to their parental full protein sequences (see text). Contigs were also enriched (to a lesser extent) for T, D, N and Q. With regard to D (Asp), phosphopeptide enrichment procedures are known to co-enrich for acidic peptides. The relatively low representation of Cys-containing phosphopeptides may have arisen from the non-use of oxidized Cysteine as a Mascot search parameter.

Kinase recognition—VPK2

Substrate preference by the Vaccinia kinase VPK2 may arise from steric factors (e.g. preference for proteins within the 7-member complex of which VPK2 is a part, proximal complexes, accessible loops within protein tertiary structures, *etc.*), or from the recognition of a target sequence. To explore the latter, all phosphorylation sites identified in the current study occurring within proteins known, from prior studies, to be VPK2 substrates (Table 1, Table S1), were collated as a set of 26 sequence segments (Fig. S3). No obvious pattern was discerned by eye within this group, other than a preponderance of Pro and Ser residues (consistent with the MV phosphoproteome as a whole, Fig. 3) and also the frequent occurrence of SSP and SP (with phosphorylation occurring at the first Ser). Any information within this set related to VPK2 recognition is accompanied, presumably, by noise from sites whose phosphorylation was VPK2-independent. To explore this, we developed an approach (described in Supplementary materials) in which each sequence segment was scored according to its distance from a consensus for all segments. After elimination of the lowest scoring segment, the process of scoring and elimination was repeated for all remaining segments. In this manner, segments were eliminated iteratively, establishing a ranking of "consensus-breaking" tendency. Combined rankings from three scoring schemes (Supplementary materials) established an aggregate score for each segment from which an ascending series of scores was generated corresponded to the original 26 segments (Fig. S4). Inflexions in the ascending series suggested four nested sub-groups of potential VPK2 substrates in addition to the starting group (Fig. S4), each sub-group representing a progressively stronger consensus. Fig. 4 shows, graphically, the sequence consensus within the initial series and sub-groups 1, 2 and 3. Sub-group 2 contained representatives of all the proteins known to be VPK2 substrates, and sub-group 3 contained representatives of all except A14L. The consensus became noticeably more information-rich by sub-group 3 with a noticeable predilection for an S, P or G residue immediately to the C-terminal side of

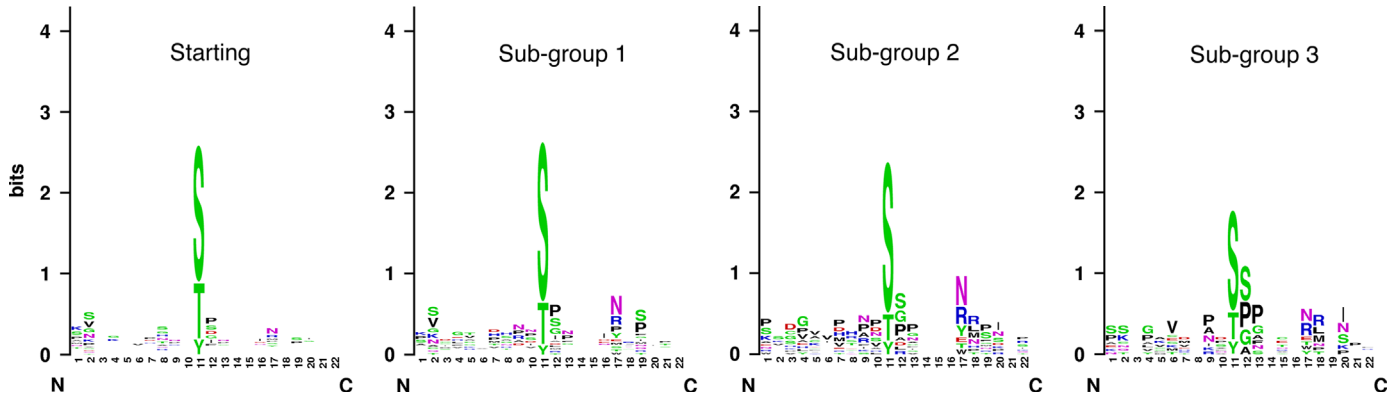

Fig. 4. Sequence Logo analysis of the regions surrounding sites of phosphorylation within known (Table 1, Table S1) VPK2 substrates. Three sub-groups show the distillation of information after progressive elimination of the most consensus-breaking sequence segments (Fig. S2).

the phosphorylation site and a preference for Pro at the subsequent residue to the C-terminal side. Additional residue preferences were also apparent (Fig. 4).

In an attempt to find any additional VPK2 substrates in the conservative MV proteome, a scoring matrix representing the consensus for sub-group 3 sites was applied globally. Using this matrix, no new sites scored higher than the segments already contributing to sub-group 3, though sites within the E4L/RP30 RNA polymerase subunit scored immediately below, along with D8L residue T243 (data not shown), raising the possibility that these may be VPK2 substrates. Using the looser sub-group 2 matrix, the E4L/RP30 and D8L sites again scored immediately below the known members of sub-group 2, along with sites in RNA polymerase subunit A5R/RP19 (data not shown), reinforcing the possibility that Vaccinia RNA polymerase is a VPK2 substrate.

Kinase recognition—All known kinase families

To infer whether specific sites in the conservative MV phosphoproteome might be attributable to cellular kinases, all sites were searched against an atlas of known kinase-family consensus sequence motifs (Miller et al., 2008). This resulted in 71 matches with a posterior probability of ≥ 0.3 (considered a stringent threshold), within which 58 MV phosphorylation sites were assigned to 12 kinase groups (some sites being assigned to multiple groups). 72% of the assignments were to just three major kinase groups (Table 2), namely CDK2/CDK3 (21 sites, covering nearly 30% of the high probability site assignments), p38 (16 sites) and CK2 (14 sites). Fig. S4 shows, graphically, the consensus for each of these three major kinase groups among the matching Vaccinia sites.

Among these groups, the CDKs (cyclin-dependent kinases) are primarily cell cycle-related in all organisms and have the consensus site [S/T*]PX[K/R] in which the starred residue is phosphorylated (Errico et al., 2010). Some Vaccinia sites were candidate CDK substrates presumably as a result of a Pro residue following the site of phosphorylation. Indeed, five members of the CDK-matching group were shared with VPK2-substrate-protein sub-groups (Fig. S2, Table 2), indicating that VPK2 might be "CDK-like" in substrate recognition (albeit the only known phylogenetic relatives of VPK2 are its homologs in other poxviruses (Punjabi and Traktman, 2005)). Alternatively, cell cycle regulators may have a role in Vaccinia virion assembly and/or release. Casein kinase 2 (CK), an S/T kinase, has also been implicated in cell cycle control and DNA repair. CK2α1 phosphorylates acidic proteins such as casein (Marin et al., 1992, Fig. S4). Two members of this group were shared with VPK2-substrate-protein sub-groups (Fig. S2, Table 2). p38 Mitogen activated protein kinases are responsive to stress stimuli such as cytokines, UV, heat/osmotic shock, apoptosis and autophagy (Sheridan et al., 2008). Vaccinia matches to p38 showed a dominating "P" after the phosphorylation site (Fig. S4).

Phosphorylation changes during virion activation

Vaccinia early transcription occurs within the infecting virus particle. *In vitro*, virus envelope removal with nonionic detergent accompanied by sulfhydryl reduction leads to the activation of virion cores for early transcription accompanied, immediately, by the phosphorylation of virion proteins (Moussatche et al., 1991). In apparent contrast to this, active VH1 phosphatase is also a requirement for early transcription, insofar as VH1-deficient virions are impaired in early transcription (Liu et al., 1995). Three of our seven MV phosphoproteome experiments addressed the phosphorylation/dephosphorylation of virion proteins upon virion activation *in vitro* (Fig. 2). Virions were treated with nonionic detergent/disulfide reducing agent in either HEPES buffer alone (in one experiment) to address virion protein dephosphorylation, or HEPES buffer supplemented with Mg.ATP (in replicate experiments) to allow intravirion kinase activation in addition to dephosphorylation. In each experiment, the soluble and core-particulate fractions remained unseparated. Each experiment employed three aliquots of purified virion, one of which remained untreated. For the dephosphorylation experiment, nonionic detergent concentrations of either 0.05% or 0.5% were used for the remaining two aliquots, reflecting conditions used in prior studies (Kates and Beeson, 1970; Moussatche and Keller, 1991; Shuman and Moss, 1989). These two conditions will be referred to as "stripped cores" and "etched cores", on the basis of AFM images indicating the gradual permeabilization of cores after virion envelope removal, with permeabilization (or "etching") being more pronounced at higher detergent concentrations (Kuznetsov et al., 2008). For each of the kinase activation experiments, the remaining two aliquots were treated with Mg.ATP at a pH of either 7.0 or 8.5 (Fig. 2). In each experiment, the activation period was terminated by dissolution and trypsinization of the three virus aliquots and differential stable isotope labeling of the resulting peptide samples. Pooling of all labeled peptides from an activation experiment was followed by phosphopeptide enrichment and nanoLC-MS/MS with precursor-level quantitation (Fig. 2). For each confidently identified phosphopeptide that was also confidently quantifiable, relative peak intensities were calculated in the peak triples arising from isotope labeling. Quantitation results are given in Table S5 after normalization as described in Table S5 legend.

Confident quantitation was achieved for only a subset of the complete set of the identified phosphopeptides in Tables S3 and S4, with the majority of the quantative information arising from

Table 2
High confidence matches of sites in the conservative MV phosphoproteome to human kinase consensus motifs. In column 3, the number of sites is given in parentheses after the protein name.

	No. of members	In Vaccinia proteins
MAJOR		
CDK2_CDK3 group	21	A11 (1), A13 (1), A4 (2), A9 (1), ETF1 (1), G2 (1) and G7 (2, one of which is in VPK2 sub-group 3), H5 (1), p4a (2), RP30 (2), F8 (1), F17 (2, in all VPK sub-groups), K4 (1) VP8 (2), VPK2 (1, in all VPK2 sub-groups)
p38 group	16	A11 (1), A13 (1), A4 (2), ETF1 (1, same site as in CDK group), G2 (1, same as in CDK group)), G7 (2, one in VPK2 sub-group 3; same sites as in CDK group), H5 (1), p4a (1), p4b (1), RP30 (2), F8 (1), F17 (2, both in all VPK2 sub-groups, 1 in CK2 group)
CK2 group	14	A11 (1), A26 (1), A4 (1), H5 (2), p4a (3), p4b (2), RP19 (2), VPK2 (1, in VPK2 sub-group 3), VF17 (1, in VPK2 sub-group 4)
TOTAL:	51	
MINOR		
NEK1_NEK5_NEK3_NEK4_NEK11_NEK2 group	5	
PKC group	4	
ATM_ATR group	3	
RCK group	2	
ACTR2_ACTR2B_TGFbR2 group	2	
DMPK group	1	
EphA7_EphA6_EphA4_EphA3_EphA5 group	1	
p70S6K group	1	
PAKB group	1	
TOTAL:	*20*	

experiment “kinase2” due to the greater intensity of precursor-level MS peaks. In our interpretation of data, all quant ratios within a ~3-fold range were discounted (regarded as “unchanged”). In this context, quantitation data, protein-by-protein, were as follows:

A6L: Protein A6L showed a strong virion kinase activation-dependent phosphorylation at residues S118 and/or S121, stronger at pH 7.0 than at pH 8.5. *A5R/RP19*: Upon virion kinase activation at pH 7.0, A5R/RP19 showed clear evidence of new phosphorylation at either S49 or S50 (Table S5). *L4R/VP8*: Phosphopeptides were quantitated containing L4R/VP8 phospho-residues S158, Y176 and S220. No significant change in phosphorylation was detected at S158 or Y176 during kinase activation, but significant phosphorylation was observed at S220 under pH 8.5 kinase activation conditions at (Table S5). L4R/VP8-S220 can be regarded, therefore, as a clear substrate for phosphorylation upon virion activation. *A14L*: A14L residue S85 was clearly phosphorylated in response to virion kinase activation, more prominently at pH 8.5 than at pH 7.0. Of the nine membrane proteins in which phosphorylation sites were confidently identified (above), only in protein A14L was the phosphorylated region considered to be internal with respect to the accompanying membrane (above). Since S85 was identified in both activation and non-activation experiments (Table S3), this site was apparently partially occupied prior to virion activation.

A13L: Upon virion kinase activation, A13L showed increased site occupancy at residues T48 (pH 7.0) and S61 (pH 8.5). Virion activation under non-kinase condition was accompanied by an over-abundance of an A13L monophosphopeptide containing residue S40, suggesting the possible dephosphorylation of another (undetected) residue within this phosphopeptide. A13L phosphorylation inside the infected cell is VPK2 and VH1-independent (Table 1).

Results for other proteins are discussed in Supplementary data (“Phosphorylation changes during activation—other proteins”).

Discussion

Prior to the current study, to the best of our knowledge, two *in vivo* sites of phosphorylation had been clearly identified among 11 reported Vaccinia phosphoproteins (Table 1) using approaches other than MS analysis. Here, in a bottom-up phosphopeptide MS analysis, we identified, conservatively, up to 189 phosphorylation sites among 48 proteins in Vaccinia mature virion preparations (Table S4). We used a “strategy of variation”, with different experiments revealing overlapping sets of phosphopeptides. No extracellular virion (EV)-specific peptides or phosphopeptides were identified, consistent with our exclusive use of MV. Our conservative dataset included phosphopeptides from nine of the 11 previously-reported Vaccinia phosphoproteins, the two exceptions being proteins I3L and E8R (Table 1, Table S4). Although these two proteins have been reported, unanimously, to be virion-associated (Table S2), E8R may be considered a phosphoprotein solely on the basis of an *in vitro* kinase assay (Table S1). Our data confirm and extend prior understanding of MV protein phosphorylation, with a few similarities and differences. Differences may arise from factors that include: (a) Phosphorylation changes during either cell harvesting, generation of cell extracts and/or virus purification; (b) phosphorylation changes during the virion lifecycle (assembly, maturation, exit, release); (c) differential sensitivity of MS and non-MS based assays; (d) incomplete protein coverage via MS; (e) prior use of context-specific anti-phospho-residue antibodies. Protein-by-protein, similarities and differences are summarized in Supplementary data (“Similarities/differences between current (MS-based) and prior phosphorylation data”).

Our conservative MV phosphoproteome contained 10 proteins not previously detected in Vaccinia MV, and with no obvious biological role therein. These included the product of a small Vaccinia ORF, YVDA (Tables S3 and S4) which is conserved between Vaccinia strains. The products of smaller ORFs may be less easily detectable by MS due to a paucity of trypsin sites, fewer choices of peptide from which to identify them and fewer phosphorylation targets. Due to our use of stringent score thresholds, most or all of the 10 proteins are likely bona fide phosphoproteins. It is unclear whether these phosphoproteins are packaged in MV at very low abundance or were trace contaminants in MV preparations. However, due to the wide abundance dynamic range of ion trap MS, the detection of trace-contaminants might be expected, even in 2x-banded MV preparations. Moreover, the detection of trace contaminants might be exacerbated, here, by phosphopeptide enrichment steps, which would tend to concentrate lower abundance peptides while depleting a background of higher abundance (non-phospho) peptides. In addition, with fast,

sensitive MS instrumentation identifying peptides in descending order of ion intensity, it is possible to dig more deeply into a proteome when it is a relatively simple one, such as that of a virion.

While the numbers of phosphates within each identified phosphopeptide is confidently ascertained on the basis of experimental peptide mass, positional location can be more ambiguous, for example where fragmentation ion series are incomplete, and/or where closely-spaced phosphorylation sites provide few fragmentation ions to distinguish candidate phosphate positions. Did the phosphopeptide positional isomers in our dataset represent alternative sites within a protein, or ambiguous localization of a single site? With the use of conservative thresholds, a liberal interpretation was adopted that positional isomers represented genuinely alternative sites unless they were the alternate progeny of a single Mascot query of a single mass spectral peak in a single spectrum. There is considerable precedent for the phosphorylation of multiple, closely-spaced sites in proteins, often by the same kinase. Examples would include the phosphorylation of ribosomal protein S6 by p70-S6 kinase at a cluster of four sites within a 10-residue stretch (Ferrari et al., 1991) and the tyrosine phosphorylation of c-Raf protein at two adjacent sites (Fabian et al., 1993). In another example, MAPKs are phosphorylated by dual specificity MKKs at both the Thr and Tyr residue within a TXY sequence (Gartner et al., 1992; Payne et al., 1991). There is also substantial precedent for the hierarchical phosphorylation of closely spaced sites within substrates by distinct kinases: Casein kinase 1 (CK1), Glycogen synthase kinase (GSK) and to a lesser extent casein kinase 2 all prefer substrates that have been "primed" at nearby sites by other kinases: Positioning requirements are kinase-specific, with CK1 preferring a pSer/pThr at position -3 relative to its own phosphorylation site, and GSKs requiring a pSer/Thr at position +4. Well-known examples of CK1 and GSK3 substrates phosphorylated in this manner include beta-catenin in the Wnt signaling pathway (Cohen and Frame, 2001).

Employing both tryptic and semi-tryptic specificity for database searches, the conservatively thresholded dataset contained a number of high confidence semi-tryptic peptides (those that were tryptic at one end only) from proteins of various classes. Non-trypsin proteolysis occurred, apparently, at some point in time between virion morphogenesis and MS analysis. Semi-tryptic peptides did not appear, or show changes of abundance, as a result of virion activation (Fig. 2, gray, data not shown). One possibility might be the "nicking" of MV proteins during virus preparation steps that exposed virus to cellular extract. Another possibility, namely source-level fragmentation of peptides at the mass spectrometer inlet could be discounted for the great majority of semi-tryptics, since only a small minority co-chromatographed with corresponding tryptics during nanoLC-MS/MS (data not shown). In most instances, semi-tryptic peptides were co-terminal (flush) at the fully-tryptic C-terminus and nested at the N-terminus, with nesting originating close to a bona fide tryptic N-terminus (Table S4). This suggests aminopeptidase activity. With aminopeptidases being zinc metalloenzymes, one possibility might be that the Vaccinia G1 zinc metallopeptidase (which is packaged) is such an enzyme and, after solubilization and release, retains some activity towards tryptic peptides during the extended trypsinization of MV proteins. This has not been tested. Irrespective of origin, the presence of semi-tryptics was an asset to the experiment, acting to confirm sites of phosphorylation within distinct background sequence environments.

Changes in phosphopeptide abundance as a result of virion activation, were measured. The resulting quantitative MS dataset was by no means complete, with a number of phosphopeptides likely below the below limit of quantitation. This area would likely benefit from a more exhaustive study. However, phosphopeptide quantitation data that were available (Table S5) proved to be generally reproducible as affirmed by multiple quantitation data points (not shown) for the same peptides in various chromatographic fractions along with various charge states/peripheral modification states contributing to the given mean values. Spectral interference issues were likely defrayed by the emptier chromatograms arising from a relatively simple starting proteome that was further simplified via phosphopeptide enrichment, contributing to reproducibility in quantitation. As a further aid in accurate quantitation, normalization procedures were employed to isolate quant changes as far as possible to the phosphate group itself.

Table 3
pH-dependent differential fold-change in phosphorylation upon activation, by protein/phosphorylation site. Alternate ratios, where indicated, arise from either different experiments or different normalization controls. Derived from Table S5.

	pH 7.0/pH 8.5	pH 8.5/pH 7.0
p4a-S743	6.85	
RP19-S49	6.81	
RP19-S50	3.65/3.68	
A6-S118/S121	1.7	
A13-T48	5.55	
A13-S61		4.10/8.43
A14-S85		4.98/9.39/8.90
VP8-S220		16.97/21.1/28.04

In each clear observation of phosphorylation changes as a result of virion kinase activation, the response was pH-biased (Table S5, Table 3) hinting at multiple pathways of intravirion protein phosphorylation. Insofar as purified VPK1 (B1 kinase) and purified VPK2 (F10 kinase) are activated at pH 9.0 (Lin et al., 1992) and pH 7.5 (Lin and Broyles, 1994) respectively, sites showing bias towards pH 8.5 and pH 7.0 activation could be VPK1 and VPK2 substrates, respectively. Within the known VPK2 target list (Fig. S2), only A14L-S85 could be quantified and, according to the above metric, it showed VPK1 bias (Table S5, Table 3). In this regard, A14L was lost from our VPK2 "order of elimination" series earlier than the other known VPK2 substrates (Fig. S3). Moreover, A14L was the only virion membrane phosphoprotein in our dataset whose phosphorylation sites were apparently internal with respect to the accompanying membrane. With regard to Vaccinia early transcription, evidence has been shown (Moussatche and Keller, 1991) for pH-biased phosphorylation of ~70 and ~80 kDa proteins during virion activation, with phosphorylation occurring primarily at pH 7.0. ~70 and ~80 kDa are consistent with the known sizes of the two VETF subunits. Albeit quantitative data were not obtained for VETF phosphopeptides in our experiments, activation-dependent phosphorylation of RNA polymerase subunits was detected, notably in A5R/RP19. According to the above metric for pH-dependence, A5R/RP19 would be a VPK2 substrate (Table 3).

Conclusions

In summary, in a deep analysis using a strategy of variation, we have unearthed up to 189 phosphorylation sites in 48 proteins in Vaccinia MV preparations with high confidence. This may represent more sites than have been found before in any virus particle. The current study provides a basis for the further investigation of phosphorylation during Vaccinia virus infection.

Materials and methods

Materials

Iodoacetamide, triethylammonium bicarbonate (TEAB), trypsin, ethyl acetate, triflouroacetic acid (TFA), glycolic acid, sodium *N*-

lauroylsarcosine, sodium deoxycholate, spermidine, NH_4OH, piperidine, CH_2O, CD_2O, $^{13}CD_2O$, $NaBH_3CN$ and $NaBD_3CN$ were from Sigma Aldrich. Tris(2-carboxyethyl)phosphine (TCEP) and KCl were from ThermoFisher Scientific, pyrrolidine was from Alfa Aesar, 4-(2-hydroxyethyl)-1-piperazineethanesulfonic acid (HEPES) was from Research Products International Corp., NaOH was from EMD Millipore, ATP was from GE Healthcare Life Sciences, $MgCl_2$ was from Calbiochem, NP40 was from US Biochemicals. Vaccinia strain WR virions were prepared and purified as described (Malkin et al., 2003). Briefly, vaccinia-infected HeLa cells were recovered by centrifugation and subjected to hypotonic lysis with dounce homogenization. After pelleting nuclei followed by sonication, virus was pelleted through a 36% sucrose cushion. The resuspended pellet was banded in a 5–40% continuous sucrose gradient, and the harvested virus was collected, recovered and banded again. Titer of the resulting MV was $\sim 4 \times 10^{10}$ PFU/mL of suspension.

Virion-level protocols

Virion activation—Uncoating only

3×50 μL (2×10^9 PFU) aliquots of purified MV suspension were centrifuged in a microfuge at full speed for 60 s, and supernatants removed. Aliquot 1 (control) was resuspended in 40 μL of 50 mM HEPES-NaOH, pH 8.5 and placed on dry ice. Aliquot 2 (for the generation of "stripped cores" (Moussatche and Keller, 1991; Shuman and Moss, 1989)) was resuspended in 20 μL of 50 mM HEPES-NaOH (pH 8.5) followed by the addition of an equal volume of 2x low-NP40 uncoating buffer (100 mM HEPES-NaOH, pH 8.5, 0.1% NP40, 80 mM TCEP). Aliquot 3 (for the generation of "Etched cores" (Kates and Beeson, 1970)) was also resuspended in 20 μL of 50 mM HEPES-NaOH (pH 8.5) followed by the addition of an equal volume of 2 × high-NP40 uncoating buffer (100 mM HEPES-NaOH, pH 8.5, 1% NP40, 80 mM TCEP). After incubation of aliquots 2 and 3 for 10 min at RT °C with occasional vortexing, aliquot 1 was thawed and supplemented with 2.8 μL of 0.5 M TCEP, then all three aliquots were supplemented with an equal volume of 2 × dissociation buffer (72 mM sodium *N*-lauroylsarcosine (NLS), 24 mM sodium deoxycholate (DOC), 10 mM TCEP, 100 mM TEAB (pH 8.0), plus 1 × phosphatase inhibitor cocktail (BioVision EZBlock Phosphatase Inhibitor Cocktail I). To solubilize proteins, all three samples were subjected to three cycles of heating at 95 °C (5 min) followed by sonication (5 min).

Virion kinase activation

3x75 μL aliquots (3×10^9 PFU) of purified MV suspension were centrifuged as above. The pellet from aliquot 1 (control) was treated as above (leaving at room temperature). Pellets from aliquots 2 and 3 were resuspended in 10 μL of 50 mM HEPES-NaOH (pH 7.0 or pH 8.5, respectively) followed by addition of an equal volume of 2 × pH 7.0 low-NP40 uncoating buffer (100 mM HEPES-NaOH, pH 7.0, 0.1% NP40, 80 mM TCEP) or 2 × pH 8.5 low-NP40 uncoating buffer (above), respectively. Incubation of aliquots 2 and 3 at room temperature for 5 min with occasional vortexing was followed by the addition of an equal volume of 2 × pH 7.0 phosphorylation buffer (50 mM HEPES-NaOH, pH 7.0, 80 mM TCEP, 2 mM ATP, 2 mM $MgCl_2$, 2 mM spermidine, 20 mM KCl) or 2 × pH 8.5 phosphorylation buffer (as above but with pH 8.5 HEPES-NaOH) to aliquots 2 and 3, respectively, and incubation at room temperature for 15 min with occasional vortexing. After incubation, aliquots were treated as above.

Other experiments ("100microL-"; "IMAC-"; "WayneLTQ")

Aliquots of Vaccinia MV suspension (50–100 μL) were centrifuged at $14{,}000 \times g$ and storage supernatant discarded. Pellets were supplemented with 1 × dissociation buffer (12 mM NLS, 12 mM DOC, 5–10 mM TCEP, 50 mM TEAB (pH 8.0)) (Masuda et al., 2008) then subjected to three cycles of heating at 95 °C (5 min) followed by sonication (5 min).

Peptide-level protocols

Trypsinization, peptide extraction and cleanup

After addition of iodoacetamide to a final concentration of 25 mM, samples were incubated in the dark for 30 min at room temperature. Protein concentrations were then determined by BCA assay (Thermo Pierce) following the manufacturer's protocol. After a 5-fold dilution with 50 mM TEAB (pH 8.0), trypsin was added at a ratio of 1:100 (w:w, enzyme:substrate). Following overnight incubation at 37 °C, a second, equivalent aliquot of trypsin was added and incubation extended for a further 3 h at 37 °C. Detergent was removed by addition of an equal volume of ethyl acetate/0.5% triflouroacetic acid (TFA) followed by vortexing for 5 min, then centrifugation at 13–14,000*g* for 30–300 s to separate phases. After discarding the organic phase, peptides were desalted using either C18 (Experiment "WayneLTQ" (Rappsilber et al., 2007)) or (for other experiments) sequential C18 and Hypercarb StageTips in P-1000 pipette tips. C18 StageTips were made with four stacks of C18 (3 M, Inc.) (Ishihama et al., 2006), and Hypercarb StageTips were made from Hypercarb beads (Thermo Scientific) layered over one stack of C8 (3 M, Inc.). In the first step of StageTip peptide cleanup, C18 stageTip-bound peptides were washed with 0.1% FA then eluted with 80% CH_3CN/0.1% formic acid (FA). Unbound peptides in the load were passed through Hypercarb stageTips, eluting with 80% CH_3CN/0.1% FA followed by 200 mM pyrrolidine/60% CH_3CN. All stageTip elutions were pooled, dried under vacuum and reconstituted in 100 μL of solution X (80% CH_3CN, 1 M glycolic acid, 5% TFA in water) if used for TiO_2 fractionation, or 1 mL of (250 mM acetic acid, 30% CH_3CN, pH 3.0) if used for IMAC, otherwise in 100 mM TEAB (pH 8.0).

Isotopic dimethyl labeling

Peptides from the previous step were isotopically labeled at N-termini/lysine sidechains with either $-CH_3$, $-CD_3$ or $-^{13}CD_3$ by mixing with either CH_2O (light), CD_2O (medium) or $^{13}CD_2O$ (heavy) prior to addition of $NaBH_3CN$ (light, medium) or $NaBD_3CN$ (heavy) (Boersema et al., 2009). After vortexing (60 min), unreacted formaldehyde was quenched with excess primary amine then excess formic acid. The three labeled samples were pooled and the mixture desalted as for C18 and Hypercarb tips (above), except using C18 Sep-Pak cartridges (200 mg, Waters) and HyperSep Hypercarb cartridges (200 mg, Thermo Scientific). Eluates were vacuum-dried then reconstituted in solution X.

Phosphopeptide enrichment, SCX

In one experiment ("WayneLTQ"), phase-separated, unlabeled peptides, after a simple C18 StageTip cleanup (above) were fractionated directly using stacked SCX-C18 StageTips with 3–6 salt cuts in the SCX fractionation step (Rappsilber et al., 2007).

Phosphopeptide enrichment, TiO_2

Titanium dioxide (TiO_2)-based enrichment columns were fabricated from either a pipette tip plugged with a section of SDB membrane (experiment "WayneLTQ") or from a 200 μL GELoader pipet tip plugged with a section of C8 membrane. TiO_2 beads (3 mg, Titansphere 5 μm, GL Sciences, Japan) were packed using 20 μL methanol (experiment "WayneLTQ") or 80% CH_3CN, 5% TFA in water as transfer solution (Jensen and Larsen, 2007), centrifuging at $14{,}000 \times g$ for 5 min to pack the beads (Sugiyama et al. (2007) with slight modification). The resulting columns were pre-

equilibrated with 100 μL of 70% CH_3CN, 29.9% lactic acid, 0.1% TFA in water (solution A), centrifuged at 400 × *g* for 5 min, repeating once (experiment "WayneLTQ"), or with 5 μL of solution X, then 20 μL of 80% CH_3CN, 1% TFA in water to wash away the glycolic acid. The equilibrated tip was loaded with peptide sample in 100 μL of solution A, followed by centrifugation at 400 × *g* for 5 min, after which beads were washed (experiment "WayneLTQ") with, sequentially, solution A (100 μL) then (80% CH_3CN, 0.1% TFA, 100 μL) to remove the lactic acid. In other experiments, beads were washed instead as for the pre-equilibration step. All experiments: Peptides were eluted by the sequential addition of 20 μL aliquots of 5% NH_4OH in water, 5% piperidine in water, then 5% pyrrolidine in water, into equivalent volumes of 10% TFA in water (Sugiyama et al., 2007). Experiment "WayneLTQ": TiO_2 fractions were individually desalted using C18 StageTips alone. Other experiments: TiO_2 fractions were individually desalted using C18 and Hypercarb StageTips as described above, but on a smaller scale in which C18 tips were fabricated by placing a C18 disk in a 200 μL micropipette tip, and HyperCarb tips were fabricated as for TiO_2, using 200 μL GELoader tips with a C8 disk inserted, and loading HyperCarb beads into the tip. After desalting, the C18 and Hypercarb elutions of each fraction were combined, evaporated to dryness, and reconstituted in 10 μL of 0.1% FA in water.

Phosphopeptide enrichment, IMAC

80 μL of a resuspended 50% slurry of PHOS-Select Iron Affinity Gel beads (Sigma Aldrich) in water was placed onto the filter of a 0.45 μm nylon Nanosep MF Centrifugal Device (Pall Life Sciences) and washed 3 × with 0.5 mL of IMAC wash solution (0.25 M acetic acid, 30% CH_3CN in water) by mixing with the beads followed by centrifugation for 30 s at 8000*g*. Desalted/reconstituted peptide sample (above) was added to beads in two aliquots, each addition followed by incubation at room temperature for 60 min with inversion mixing then centrifugation for 30 s at 8000*g*. Beads were then washed once with 0.5 mL of IMAC wash solution and once with H_2O, each wash followed by centrifugation for 30 s at 8000*g*. Peptides were eluted with 0.5 mL of 0.4 M NH_4OH, 30% CH_3CN in water then 0.5 mL of 0.2 M sodium phosphate (pH 8.4), in water. For each elution, beads were incubated for 5 min with inversion then centrifuged for 30 s at 8000*g*. Eluates were acidified immediately then desalted individually, as described above ("Phosphopeptide enrichment, TiO_2").

NanoLC-MS/MS, database searching and data processing

Phosphopeptides were analyzed on either the LTQ Classic mass spectrometer with CID fragmentation or the LTQ Velos Pro mass spectrometer with ETD capability. In either case, samples were injected to a 75 μm or 100 μm × 150 mm C18-packed nanospray tip in 2–5% CH_3CN, 0.1% formic acid, eluting during nanospray ESI-LC-MS/MS with a gradient of 2–95% CH_3CN in 0.1% formic acid, over 3 h. Instrument methods for the LTQ Classic picked the 3–7 most intense ions in precursor spectra in the context of dynamic exclusion, for CID fragmentation via either multistage activation or neutral loss-triggered MS3. Instrument methods for the LTQ Velos Pro picked the 10 most intense multiply-charged ions in precursor spectra in the context of dynamic exclusion, for alternating pairs of MS2 scans with the alternating MS2 scan pairs employing either HCD/ETD or CID/ETD fragmentation modes. ETD scans employed supplemental activation. For quantitative (virion activation) experiments, data were acquired in profile mode, and for other experiments in centroid mode.

NanoLC-MS/MS spectral raw files were processed into individual peaklist (.mgf) files (or into a single merged.mgf for all raw files from experiment "WayneLTQ") using Mascot Distiller 2.4 (Matrix Science). Mascot Server 2.4 (Matrix Science) was used for peaklist searches against three databases, namely the target database (SwissProt 2012_03, selecting Vaccinia WR or human+Vaccinia taxonomy), a database of common contaminants, and a decoy database of random sequences of equivalent composition, selecting either tryptic or semi-tryptic specificity and up to 1 missed cleavage (Table S6). A single fixed modification was selected, namely cysteine carbamidomethylation. Variable modifications comprised methionine oxidation, deamidated (NQ), serine/threonine phosphorylation and tyrosine phosphorylation. Precursor mass tolerance was 0.25 Da allowing 2+/3+ charge, MS/MS fragment mass tolerance was 0.5 Da, $^{13}C=0$ (see Table S6 for full listing of search, report and export settings). Mascot Server search reports were re-thresholded by adjusting FDR (decoy:target hits ratio) to either 1% or 5% before generation of protein- and peptide-level exports (Table S6). The resulting protein- and peptide-level exports were reformatted, sorted, merged, filtered, condensed, enumerated, interpreted, and figures were generated, using in-house software (Supplementary methods).

For confidence in phosphosite localization, Mascot Server 2.4 provided "site_analysis" confidence (SAC) values (for SAC, Mascot exports adopted the header "pep_var_mod_conf", Table S3) following the method of ref. (Savitski et al., 2011). SAC values equated most simply to $1-(10\backslash widehat(-M\times V))\times 100\%$, where M is the Mascot Delta score ("MD-Score" of ref. (Savitski et al., 2011)) and V is nominally 0.1 (equating an MD-score of 10 to a confidence of 90%). However, in practice, V was iterated during each calculation to achieve a sum of 100% for the SAC values corresponding to the MD-scores of the ten best peptide-spectrum matches.

For precursor-level quantitation (virion activation) experiments, database searching employed exclusive modifications comprising heavy, intermediate, and light dimethyl labels on peptide lysine side chains and N termini (Boersema et al., 2009) and quant ratios were calculated in Mascot Distiller after spectral peak fitting and peak area determination for the fitted model. Data from Mascot Distiller were exported using significance thresholds corresponding to 1% FDR (as employed in Mascot Server, above). Exported quant values were treated and analyzed using in-house software as described (Chou et al., 2012), except that each distinct peptide species was considered to be quantitatively independent (as opposed to grouping/averaging by protein accession). Quant ratios were discarded for all peptide species without multiple quant determinations, and any outlying quant values among multiple determinations were validated visually then discarded if necessary (Chou et al., 2012). Final quant ratio values adopted the geometric mean of individual determinations.

Acknowledgments

This work received no financial support.

Appendix A. Supporting information

Supplementary data associated with this article can be found in the online version at http://dx.doi.org/10.1016/j.virol.2014.01.012.

References

Banham, A.H., Leader, D.P., Smith, G.L., 1993. Phosphorylation of ribosomal proteins by the vaccinia virus B1R protein kinase. FEBS Lett. 321 (1), 27–31.

Banham, A.H., Smith, G.L., 1992. Vaccinia virus gene B1R encodes a 34-kDa serine/threonine protein kinase that localizes in cytoplasmic factories and is packaged into virions. Virology 191 (2), 803–812.

Betakova, T., Wolffe, E.J., Moss, B., 1999. Regulation of vaccinia virus morphogenesis: phosphorylation of the A14L and A17L membrane proteins and C-terminal truncation of the A17L protein are dependent on the F10L kinase. J. Virol. 73 (5), 3534–3543.

Black, E.P., Moussatche, N., Condit, R.C., 1998. Characterization of the interactions among vaccinia virus transcription factors G2R, A18R, and H5R. Virology 245, 313–322.

Boersema, P.J., Raijmakers, R., Lemeer, S., Mohammed, S., Heck, A.J., 2009. Multiplex peptide stable isotope dimethyl labeling for quantitative proteomics. Nat. Protoc. 4 (4), 484–494.
Brown, N.G., Nick Morrice, D., Beaud, G., Hardie, G., Leader, D.P., 2000. Identification of sites phosphorylated by the vaccinia virus B1R kinase in viral protein H5R. BMC Biochem. 1, 2.
Chalkley, R.J., Clauser, K.R., 2012. Modification site localization scoring: strategies and performance. Mol. Cell Proteomics 11 (5), 3–14.
Chou, W., Ngo, T., Gershon, P.D., 2012. An overview of the vaccinia virus "Infectome": a survey of the proteins of the poxvirus-infected cell. J. Virol. 86 (3), 1487–1499.
Chung, C.S., Chen, C.H., Ho, M.Y., Huang, C.Y., Liao, C.L., Chang, W., 2006. Vaccinia virus proteome: identification of proteins in vaccinia virus intracellular mature virion particles. J. Virol. 80 (5), 2127–2140.
Cohen, P., Frame, S., 2001. The renaissance of GSK3. Nat. Rev. Mol. Cell Biol. 2 (10), 769–776.
Condit, R.C., Moussatche, N., Traktman, P., 2006. In a nutshell: structure and assembly of the vaccinia virion. In: Maramorosch, K., Shatkin, J. (Eds.), Advances in Virus Research, vol. 66. Elsevier, pp. 31–124.
da Fonseca, F.G., Weisberg, A.S., Caeiro, M.F., Moss, B., 2004. Vaccinia virus mutants with alanine substitutions in the conserved G5R gene fail to initiate morphogenesis at the nonpermissive temperature. J. Virol. 78 (19), 10238–10248.
Derrien, M., Punjabi, A., Khanna, M., Grubisha, O., Traktman, P., 1999. Tyrosine phosphorylation of A17 during vaccinia virus infection: involvement of the H1 phosphatase and the F10 kinase. J. Virol. 73 (9), 7287–7296.
Errico, A., Deshmukh, K., Tanaka, Y., Pozniakovsky, A., Hunt, T., 2010. Identification of substrates for cyclin dependent kinases. Adv. Enzyme Regul. 50 (1), 375–399.
Fabian, J.R., Daar, I.O., Morrison, D.K., 1993. Critical tyrosine residues regulate the enzymatic and biological activity of Raf-1 kinase. Mol. Cell Biol. 13 (11), 7170–7179.
Fermin, D., Walmsley, S.J., Gingras, A.C., Choi, H., Nesvizhskii, A.I., 2013. LuciPHOr: algorithm for phosphorylation site localization with false localization rate estimation using target-decoy approach. Mol. Cell Proteomics
Ferrari, S., Bandi, H.R., Hofsteenge, J., Bussian, B.M., Thomas, G., 1991. Mitogen-activated 70K S6 kinase. Identification of *in vitro* 40S ribosomal S6 phosphorylation sites. J. Biol. Chem. 266 (33), 22770–22775.
Gartner, A., Nasmyth, K., Ammerer, G., 1992. Signal transduction in Saccharomyces cerevisiae requires tyrosine and threonine phosphorylation of FUS3 and KSS1. Genes Dev. 6 (7), 1280–1292.
Guan, K.L., Broyles, S.S., Dixon, J.E., 1991. A Tyr/Ser protein phosphatase encoded by vaccinia virus. Nature 350 (6316), 359–362.
Howard, S.T., Smith, G.L., 1989. Two early vaccinia virus genes encode polypeptides related to protein kinases. J. Gen. Virol. 70 (Pt 12), 3187–3201.
Hunter, T., 1998. The Croonian Lecture 1997. The phosphorylation of proteins on tyrosine: its role in cell growth and disease. Philos. Trans. R Soc. London B Biol. Sci. 353 (1368), 583–605.
Hunter, T., Sefton, B.M., 1980. Transforming gene product of Rous sarcoma virus phosphorylates tyrosine. Proc. Nat. Acad. Sci. U.S.A. 77 (3), 1311–1315.
Ibrahim, N., Wicklund, A., Jamin, A., Wiebe, M.S., 2013. Barrier to autointegration factor (BAF) inhibits vaccinia virus intermediate transcription in the absence of the viral B1 kinase. Virology 444 (1–2), 363–373.
Ishihama, Y., Rappsilber, J., Mann, M., 2006. Modular stop and go extraction tips with stacked disks for parallel and multidimensional peptide fractionation in proteomics. J. Proteome Res. 5 (4), 988–994.
Jacob, T., Van den Broeke, C., Favoreel, H.W., 2011. Viral serine/threonine protein kinases. J .Virol. 85 (3), 1158–1173.
Jensen, S.S., Larsen, M.R., 2007. Evaluation of the impact of some experimental procedures on different phosphopeptide enrichment techniques. Rapid Commun. Mass Spectrom. 21 (22), 3635–3645.
Kates, J., Beeson, J., 1970. Ribonucleic acid synthesis in vaccinia virus I. The mechanism of synthesis and release of RNA in vaccinia cores. J. Mol. Biol. 50, 1–18.
Kleiman, J., Moss, B., 1973. Protein kinase activity from vaccinia virions: solubilization and separation into heat-labile and heat-stable components. J. Virol. 12 (4), 684–689.
Kleiman, J.H., Moss, B., 1975a. Characterization of a protein kinase and two phosphate acceptor proteins from vaccinia virions. J. Biol. Chem. 250 (7), 2430–2437.
Kleiman, J.H., Moss, B., 1975b. Purification of a protein kinase and two phosphate acceptor proteins from vaccinia virions. J. Biol. Chem. 250 (7), 2420–2429.
Koksal, A.C., Nardozzi, J.D., Cingolani, G., 2009. Dimeric quaternary structure of the prototypical dual specificity phosphatase VH1. J. Biol. Chem. 284 (15), 10129–10137.
Kuznetsov, Y., Gershon, P.D., McPherson, A., 2008. Atomic force microscopy investigation of vaccinia virus structure. J. Virol. 82 (15), 7551–7566.
Lin, S., Broyles, S.S., 1994. Vaccinia protein kinase 2: a second essential serine/threonine protein kinase encoded by vaccinia virus. Proc. Nat. Acad. Sci. U.S.A. 91 (16), 7653–7657.
Lin, S., Chen, W., Broyles, S.S., 1992. The vaccinia virus B1R gene product is a serine/threonine protein kinase. J. Virol. 66 (5), 2717–2723.
Liu, K., Lemon, B., Traktman, P., 1995. The dual-specificity phosphatase encoded by vaccinia virus, VH1, is essential for viral transcription *in vivo* and *in vitro*. J. Virol. 69 (12), 7823–7834.
Malkin, A.J., McPherson, A., Gershon, P.D., 2003. Structure of intracellular mature vaccinia virus visualized by *in situ* atomic force microscopy. J. Virol. 77 (11), 6332–6340.
Mann, M., Ong, S.E., Gronborg, M., Steen, H., Jensen, O.N., Pandey, A., 2002. Analysis of protein phosphorylation using mass spectrometry: deciphering the phosphoproteome. Trends Biotechnol. 20 (6), 261–268.
Marin, O., Meggio, F., Draetta, G., Pinna, L.A., 1992. The consensus sequences for cdc2 kinase and for casein kinase-2 are mutually incompatible. A study with peptides derived from the beta-subunit of casein kinase-2. FEBS Lett. 301 (1), 111–114.
Masuda, T., Tomita, M., Ishihama, Y., 2008. Phase transfer surfactant-aided trypsin digestion for membrane proteome analysis. J. Proteome Res. 7 (2), 731–740.
Meng, X., Embry, A., Sochia, D., Xiang, Y., 2007. Vaccinia virus A6L encodes a virion core protein required for formation of mature virion. J. Virol. 81 (3), 1433–1443.
Mercer, J., Traktman, P., 2005. Genetic and cell biological characterization of the vaccinia virus A30 and G7 phosphoproteins. J. Virol. 79, 7146–7161.
Miller, M.L., Jensen, L.J., Diella, F., Jorgensen, C., Tinti, M., Li, L., Hsiung, M., Parker, S. A., Bordeaux, J., Sicheritz-Ponten, T., Olhovsky, M., Pasculescu, A., Alexander, J., Knapp, S., Blom, N., Bork, P., Li, S., Cesareni, G., Pawson, T., Turk, B.E., Yaffe, M.B., Brunak, S., Linding, R., 2008. Linear motif atlas for phosphorylation-dependent signaling. Sci. Signal 1 (35), ra2.
Moussatche, N., Keller, S.J., 1991. Phosphorylation of vaccinia virus core proteins during transcription *in vitro*. J. Virol. 65 (5), 2555–2561.
Nezu, J., Oku, A., Jones, M.H., Shimane, M., 1997. Identification of two novel human putative serine/threonine kinases, VRK1 and VRK2, with structural similarity to vaccinia virus B1R kinase. Genomics 45 (2), 327–331.
Paoletti, E., Moss, B., 1972. Protein kinase and specific phosphate acceptor proteins associated with vaccinia virus cores. J. Virol. 10 (3), 417–424.
Payne, D.M., Rossomando, A.J., Martino, P., Erickson, A.K., Her, J.H., Shabanowitz, J., Hunt, D.F., Weber, M.J., Sturgill, T.W., 1991. Identification of the regulatory phosphorylation sites in pp42/mitogen-activated protein kinase (MAP kinase). EMBO J. 10 (4), 885–892.
Punjabi, A., Traktman, P., 2005. Cell biological and functional characterization of the vaccinia virus F10 kinase: implications for the mechanism of virion morphogenesis. J. Virol. 79 (4), 2171–2190.
Rappsilber, J., Mann, M., Ishihama, Y., 2007. Protocol for micro-purification, enrichment, pre-fractionation and storage of peptides for proteomics using StageTips. Nat. Protoc. 2 (8), 1896–1906.
Rempel, R.E., Traktman, P., 1992. Vaccinia virus B1 kinase: phenotypic analysis of temperature-sensitive mutants and enzymatic characterization of recombinant proteins. J. Virol. 66 (7), 4413–4426.
Resch, W., Hixson, K.K., Moore, R.J., Lipton, M.S., Moss, B., 2007. Protein composition of the vaccinia virus mature virion. Virology 358 (1), 233–247.
Resch, W., Weisberg, A.S., Moss, B., 2005. Vaccinia virus nonstructural protein encoded by the A11R gene is required for formation of the virion membrane. J. Virol. 79 (11), 6598–6609.
Rodriguez, J.R., Risco, C., Carrascosa, J.L., Esteban, M., Rodriguez, D., 1997. Characterization of early stages in vaccinia virus membrane biogenesis: implications of the 21-kilodalton protein and a newly identified 15-kilodalton envelope protein. J. Virol. 71 (3), 1821–1833.
Rosemond, H., Moss, B., 1973. Phosphoprotein component of vaccinia virions. J. Virol. 11 (6), 961–970.
Salmons, T., Kuhn, A., Wylie, F., Schleich, S., Rodriguez, J.R., Rodriguez, D., Esteban, M., Griffiths, G., Locker, J.K., 1997. Vaccinia virus membrane proteins p8 and p16 are cotranslationally inserted into the rough endoplasmic reticulum and retained in the intermediate compartment. J. Virol. 71 (10), 7404–7420.
Sarov, I., Joklik, W.K., 1972. Studies on the nature and location of the capsid polypeptides of vaccinia virions. Virology 50 (2), 579–592.
Savitski, M.M., Lemeer, S., Boesche, M., Lang, M., Mathieson, T., Bantscheff, M., Kuster, B., 2011. Confident phosphorylation site localization using the Mascot Delta Score. Mol. Cell Proteomics 10 (2) (M110 003830).
Senkevich, T.G., Koonin, E.V., Moss, B., 2009. Predicted poxvirus FEN1-like nuclease required for homologous recombination, double-strand break repair and full-size genome formation. Proc. Nat. Acad. Sci. U.S.A. 106 (42), 17921–17926.
Sheridan, D.L., Kong, Y., Parker, S.A., Dalby, K.N., Turk, B.E., 2008. Substrate discrimination among mitogen-activated protein kinases through distinct docking sequence motifs. J. Biol. Chem. 283 (28), 19511–19520.
Shuman, S., Moss, B., 1989. Bromouridine triphosphate inhibits transcription termination and mRNA release by vaccinia virions. J. Biol. Chem. 264 (35), 21356–21360.
Sugiyama, N., Masuda, T., Shinoda, K., Nakamura, A., Tomita, M., Ishihama, Y., 2007. Phosphopeptide enrichment by aliphatic hydroxy acid-modified metal oxide chromatography for nano-LC-MS/MS in proteomics applications. Mol. Cell Proteomics 6 (6), 1103–1109.
Szajner, P., Jaffe, H., Weisberg, A.S., Moss, B., 2004. A complex of seven vaccinia virus proteins conserved in all chordopoxviruses is required for the association of membranes and viroplasm to form immature virions. Virology 330, 447–459.
Szajner, P., Weisberg, A.S., B., M., 2004. Evidence for an essential catalytic role of the F10 protein kinase in vaccinia virus morphogenesis. J. Virol. 78 (1), 257–265.
Szajner, P., Weisberg, A.S., Moss, B., 2004. Physical and functional interactions between vaccinia virus F10 protein kinase and virion assembly proteins A30 and G7. J. Virol. 78 (1), 266–274.
Traktman, P., Anderson, M.K., Rempel, R.E., 1989. Vaccinia virus encodes an essential gene with strong homology to protein kinases. J. Biol. Chem. 264 (36), 21458–21461.
VanSlyke, J.K., Franke, C.A., Hruby, D.E., 1991. Proteolytic maturation of vaccinia virus core proteins—identification of a conserved motif at the N termini of the 4b and 25K virion proteins. J. Gen. Virol. 72, 411–416.

VanSlyke, J.K., Whitehead, S.S., WIlson, E.M., Hruby, D.E., 1991. The multi-step proteolytic maturation pathway utilized by vaccinia virus P4a protein: a degenerate conserved cleavage motif within core proteins. Virology 183, 467–478.
Wang, S., Shuman, S., 1995. Vaccinia virus morphogenesis is blocked by temperature-sensitive mutations in the F10 gene, which encodes protein kinase 2. J. Virol. 69 (10), 6376–6388.
Yoder, J.D., Chen, T.S., Gagnier, C.R., Vemulapalli, S., Maier, C.S., Hruby, D.E., 2006. Pox proteomics: mass spectrometry analysis and identification of Vaccinia virion proteins. Virol. J. 3 (1), 10.